Crash and Vibration Analysis of rotors in a Roots Vacuum Booster

Manuel Roth[1], Stefan Kolling[2]
[1] Pfeiffer Vacuum GmbH, R&D Backing Pumps, Asslar, Germany
[2] Giessen University of Applied Sciences, Laboratory of Mechanics, Germany

Summary:

The dynamic behaviour of a roots vacuum booster with two rotors is presented. The dynamic response of the structure is, thereby, investigated using an explicit analysis for the crash behaviour and an implicit analysis for the vibration behaviour.

Typically the rotors run from 3000rpm to 3600rpm, but because of a desired rise in power density it is necessary to design rotors for operation at 6000rpm. With increasing rotational velocity the dynamic loading and the inertial forces increase as well. To face this challenge a rotor with less weight was developed. To come to a conclusion about impact behaviour, dynamic deformation and bearing-reactions a crash between the two rotors has been simulated. These results are compared with another rotor which show the potential of weight reduction.

The rotor and shaft are made from cast iron. For the material model in the crash analysis, a comparison between Mat_Piecewise_Linear_Plasticity and Mat_Gurson_JC has been accomplished. To consider triaxiality a vonMises yield locus is used together with the Johnson-Cook failure criterion in Mat_Gurson_JC, i.e. damage and its accumulation has been neglected, see [4] and [7].

In an implicit eigenvalue analysis the eigenfrequencies are determined. Roots pumps are assembled in industrial installations, where it is necessary to know the appearing natural frequencies to avoid resonance vibrations.

Keywords:

roots vacuum pump, iron casting, triaxiality, failure, Johnson-Cook, explicit/implicit, eigenvalue analysis

1 Introduction

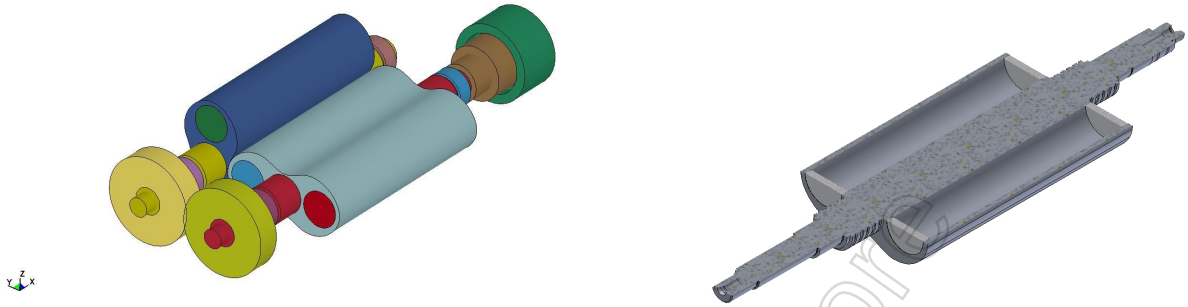

Figure 1: The two rotors and the alpha-rotor in cut

Pfeiffer Vacuum develops and maintains vacuum-pumps and vacuum-measurement. Since the beginning of the 20th century, Pfeiffer Vacuum has been an innovative company.

1.1 Application of vacuum and a roots pump

Vacuum-pumps are used in many industrial applications, especially in the coating industry. Currently vacuum-pumps are also used to manufacture photovoltaic systems and are important to the pharmaceutical-industry and research-institutes.

Many industrial installations run during a few months or years without being stopped. So the equipment has to be very robust. The process including a vacuum system is leak-proof. If a malfunction of the pump happens in such an installation, a leak in the system has to be avoided consequently. The housing in special has to stay leakproof. The energies occuring in a crash, that is a contact of the rotors, have thus to be absorbed internally by deformation of the rotors and not by rupture of the housing. Thinking of adhesive and explosiv gas which is transported, this is an important safety factor.

With a roots pump, very large pumping speeds are possible. The highest level of vacuum a roots vacuum pump that can be achieved is approximately 10^{-4}mbar, which is located in the so-called ”high vacuum” region. A roots pump does not work as a stand-alone-pump, but always is in need of a backing-pump to relieve pressure on the fore-vacuum-flange. The principal function of a roots pump is the same as the one of a roots booster. Two rotors roll with contrary sense of rotation on another without contact. The main rotor is attached to the motor with a coupler. The secondary rotor is synchronized using a gear train located at the head of the motor.

The rotors run at 3000rpm to 3600rpm and are exposed to a temperature of 150°C. In many instances the customer wishes to achieve a higher power density. To encounter this, Pfeiffer Vacuum maintains pumps with higher rotational velocity up to 6000rpm. This means a higher load to the bearings and also risen energy at a crash-event. To meet this challenge, a rotary-piston with less weight has been developed.

As material for shaft and rotary-piston iron casting is used. The crash simulation considers two versions of rotors with two different rotor geometries. The one for 3000rpm operation is processed with a solid piston and will be called the beta-piston further on. The other one for 6000rpm operation includes axial holes on each side of the shaft and will be called the alpha-piston.

During the analysis of a crash event the question of material modelling appears. In this paper two material models regarding their failure criteria are discussed. In additional to the crash simulation an implicit eigenvalue analysis has been taken into account to investigate the natural frequencies in order to avoid resonance vibrations during operation of the rotor.

2 Crash Event

2.1 Model Setup

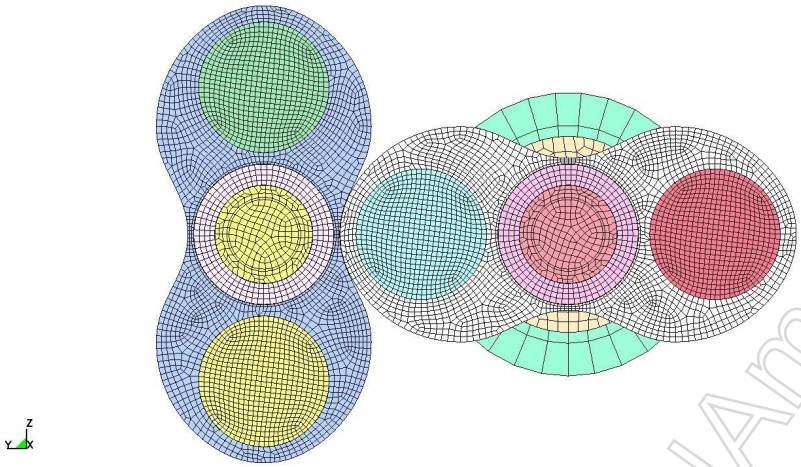

Figure 2: mesh of the alpha rotors

In this section the model setup is presented, including two different material models concerning their failure criterion.

2.1.1 Finite Element Mesh and Boundary Conditions

The rotors are mounted by ball bearings on each side of the pistons. The ball bearings are modelled as a simple ring which does not touch the shaft at time $t = 0$. On the external side of the rings, SPCs fix them. The rotors are hold into position by contact definitions. A comparison to model the ball bearings as constrained_nodal_rigid_bodys using constrained_joint_cylindrical definitions has been accomplished. The effect to the crash-behaviour did not seem to be crucial, so the way of modelling with contact definitions has been chosen.

For meshing a hexa-mesh with high quality is used as shown in fig. 2. The beta-model consists of 140'000 elements. It is possible to economize the weight of the two rotors for 22% and referred to the pistons reduce for 40%.

The Automatic-Single-Surface algorithm is used for the required contact conditions. It is applied on the entire model, except of the gearing.

2.1.2 Material Models

The piston and the shaft are made of cast iron. The foundry provided material properties and a stress–strain curve of a uni-axial tensile test. As material model for the casting parts we use MAT_Gurson_JC (material no. 120). Coupler and gearing are modelled as rigid bodies using material no. 20.

The stress–strain curve from the foundry has been converted to a vonMises-stress over plastic-strain curve. This is shown in fig. 3. Like it is well known from MAT_Piecewise_Linear_Plasticity (material no. 24) this curve is directly used in the material card without any parameter identification.

Failure is considered in MAT_024 as plastic strain at failure, i.e. dependency of state of stress is not available. That means the failure strain ε_f always got the same value independently of the triaxiality that may be defined by

$$\chi := \frac{p}{\sigma_{vm}}, \tag{1}$$

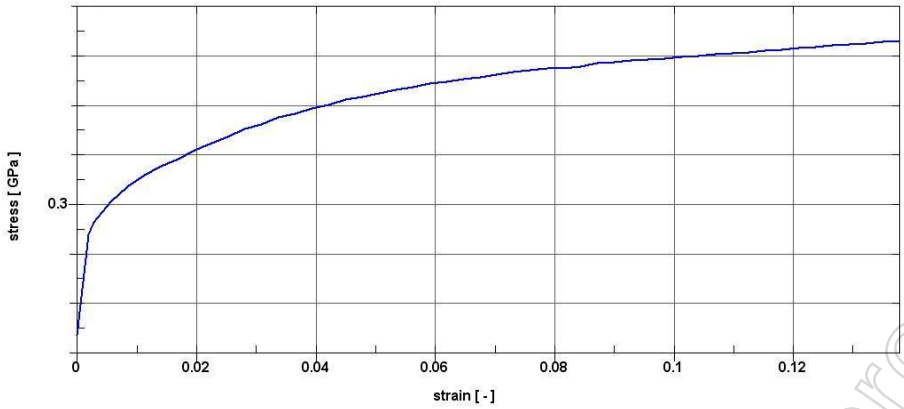

Figure 3: vonMises stress versus plastic Strain

where p is the hydrostatic pressure and σ_{vm} denotes the equivalent (vonMises) stress.

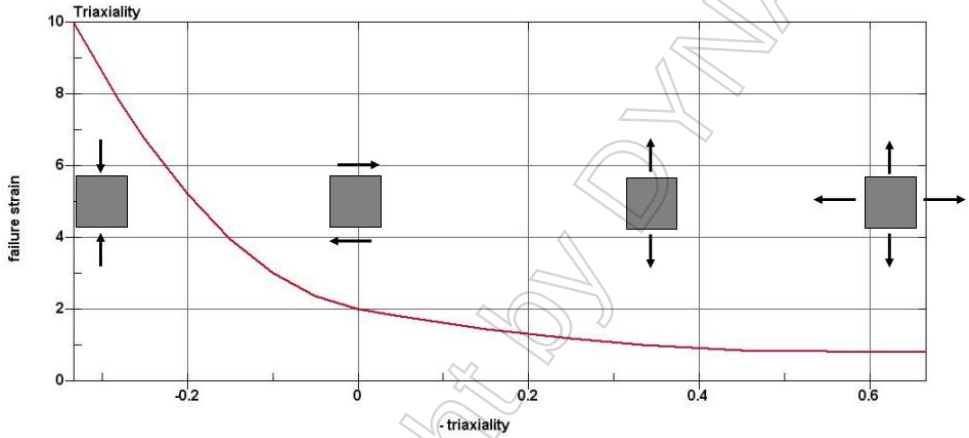

Figure 4: failure strain over triaxiality

Thus, the failure criterion in MAT_024 works only for uniaxial tension is, withal, strain rate independent. For polyaxial stress values like in the present case, an advanced failure model is needed. MAT_Gurson_JC uses the very popular failure criterion which is given by Johnson and Cook:

$$\varepsilon_f = [d_1 + d_2 \exp(d_3 \chi)] \left(1 + d_4 \ln \frac{\dot{\varepsilon}}{\dot{\varepsilon}_0}\right), \tag{2}$$

where $d_1 \ldots d_4$ are constants and χ is the triaxiality in (1). In contrast to Mat_024, the strain rate and the state of stress is also being considered. Fig. 4 shows the failure strain ε_f over the triaxiality χ. This curve is given on the LCJC-Flag of the Mat_120 card. The failure strain for uniaxial tension is given as a curve of failure strain ε_f over element length l_e. This curve is referenced at the LCDAM-Flag.

Mat_Gurson_JC is also able to take damage into account. Gurson's damaged yield function is defined as

$$\Phi = \frac{\sigma_{vm}^2}{\sigma_Y^2} + 2q_1 f^* \cosh\left(\frac{3q_2 p}{2\sigma_Y}\right) - 1 - (q_1 f^*)^2 = 0, \tag{3}$$

where σ_{vm} is the equivilent (vonMises) stress, σ_y the actual yield stress in the matrix material, p denotes the hydrostatic pressure and f^* is the effective void volume fraction.

Iron casting fails with a brittle failure-behaviour. This takes place without any pronounced necking and damage. So the parameters are set in such a way that Gurson's yield function (3) acts like a vonMises stress.

The choice of the material model has a big influence on the required solving time. Using Mat_024 the total CPU time is less than one hour where the computation time increases to nearly five hours using Mat_120.

2.2 Simulation

The rotors roll on another without contact. Also to the housing, there is no contact. The gas is forwarded by the pistons and only a little internal leakage exists because of the gaps. It is no problem to pump contaminated gas, but it happens, that one of the pistons get in touch with the housing and is decelerated or even stops. This can happen because of dust during a long term operation or a abrupt appearance of to coarse particles.

In this simulation, a crash event is accomplished, where the rotors knock on each other with a rotational velocity of 1500rpm. So each on runs with half of the maximum total velocity. This is the worst case. Generally the rotors are expected to reduce their velocity in the pre-phase of a crash event.

The crash event takes place with one rotor horizontal and the other one vertical with a angle of 90°, as it is shown by fig. 1. That leads to contact of two different areas at the two pistons. The vertical one gets in touch at an inner area where the circumferential velocity is lower and the stiffness is high. The horizontal piston touches the piston with high circumferential velocity and a lower stiffness. An alternatively set would be both pistons in 45°-position. Then areas with nearly similar velocitys and stiffnesses get in touch with each other. Further on the 90°-position will be discussed.

2.2.1 Crash Behaviour

The effect of triaxiality has been pointed out in section 2.1. Fig. 5 shows the history plot of the triaxiality χ in an element. That makes clear, that compression is dominant in the crash area of the piston.

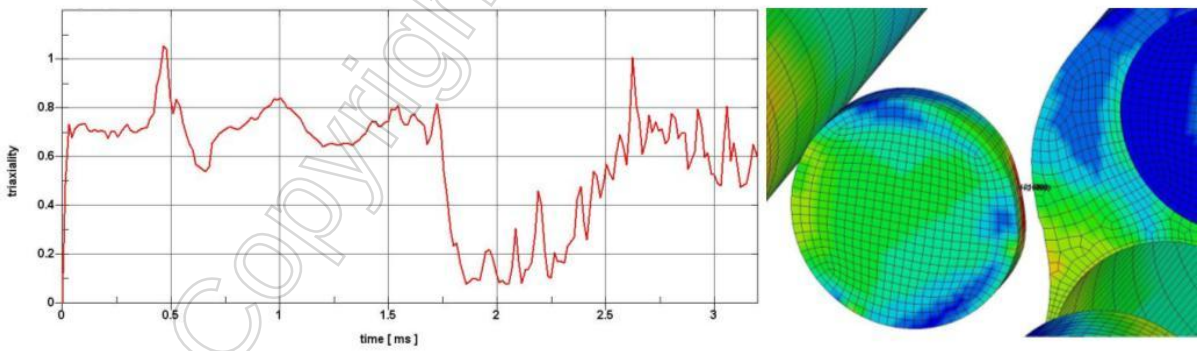

Figure 5: triaxiality over time in an element

Fig 6 shows the crash event of a piston modelled with Mat_024. There elements fail and a crack appears. As it is obvious in fig. 7 the piston does not fail using Mat_120. This matches with the real behaviour of the piston.

Fig. 7 and 8 show the plastic strain. The pistons of the beta-rotor show a nearly similar plastic strain value and a low deformation. The pistons of the alpha-rotor show a different plastic strain value. One of the rotors has got a higher deformation and a higher strain as the other one. This can also be seen at the energy plot, which is discussed below.

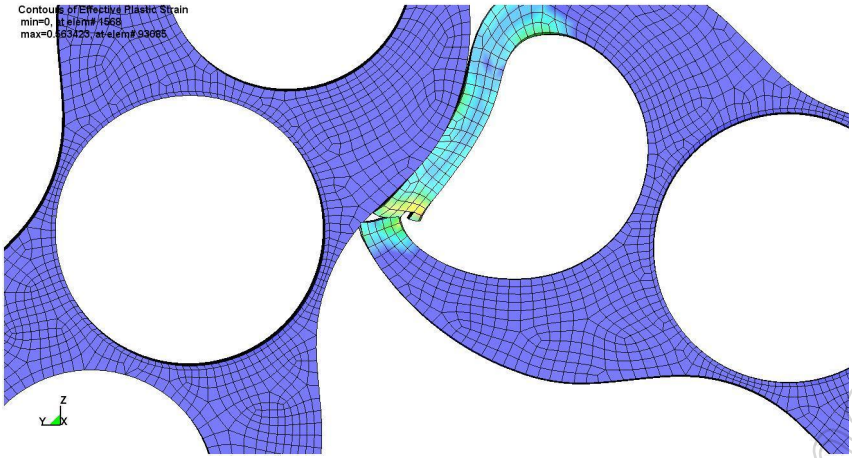

Figure 6: alpha-rotor Plastic Strain Mat_024

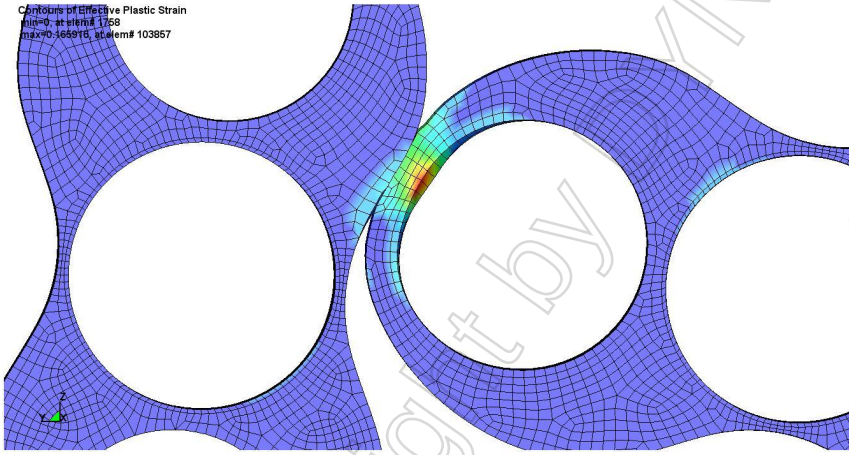

Figure 7: alpha-rotor Plastic Strain Mat_120

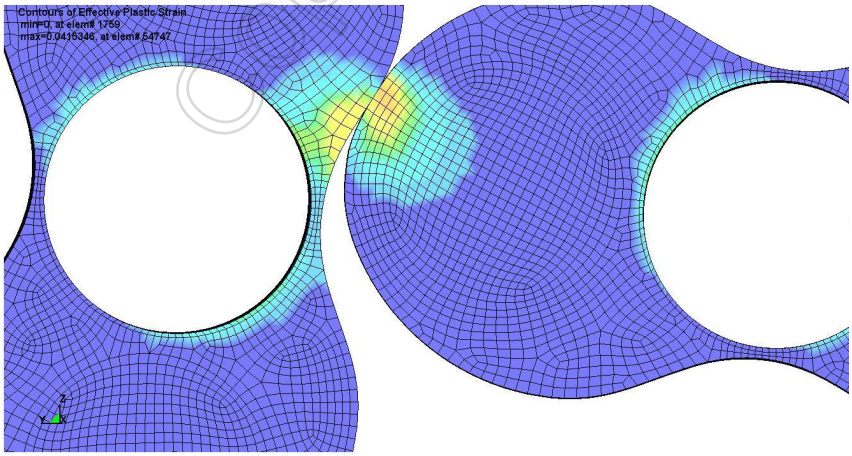

Figure 8: beta-rotor Plastic Strain

2.2.2 Energy Absorbtion

Reducing the mass of moveable parts also means a reduction of the kinetic energy and thereby a reduction of the total energy. Considering this the total energy of the alpha-piston is lower than of the beta-piston. So it is clear that the sub-energies are lower as well. This shows fig. 9.

Every component of the rotors absorbs energy. The main part of it is absorbed by the two shafts and pistons. The more the pistons deforms the less the shafts bend. High deformation of the shafts mean high forces to the bearings at the same time. So a high deformation of the pistons is desired.

To compare the two rotors the internal energies have been scaled to its specific total energy. Fig. 10 and 11 show the internal energies, which are absorbed by the two pistons and the two shafts. The internal energy is defined as

$$W_{int} = \int_V \sigma : \varepsilon dV \,, \tag{4}$$

where σ is the actual local stress, ε the actual local strain and V the current volume of the entire system.

In both cases, the shafts absorbs more energy than the pistons. The deflexion of the shafts is huge and the forces onto the bearings as well. The pistons hold a lower energy absorption. Compared to each other the beta-pistons hold a nearly similar energy absorption. The pistons of the alpha-rotor hold a different energy absorption.

The internal energy, which is absorbed by the alpha-shafts is lower than of the beta-shafts. Therefore the sum of energy, which is absorbed by deformation at the pistons is higher.

3 Eigenvalue Analysis

Roots pumps get assembled in industrial installations. These include a lot more machines, and every one of them has got movable components. This leads to a wide range of frequencies. To reach high accuracies and process reliability one has to know the single frequencies and the frequency spectrum of the installation.

Pfeiffer Vacuum developed methods to analyze their pumps. In a lot of experiments knowledge at this area is gained. To save costs, the frequency analysis are more and more part of the development process.

3.1 Model Setup

LS-DYNA is an explicit code which can not only be used for crash analysis but it is able to compute implicit analysis as well.

The IMFLAG of the Control_Implicit_General changes the mode from explicit to implicit. The Control_Implicit_Eigenvalue card defines the conditions for the eigenvalue analysis. As the MAT_Gurson_JC material is not implemented for implicit analysis, MAT_Simplified_Johnson_Cook (material no. 098) is used instead. This is, however, absolutely equal because linear elasticity is considered only. The material models behave similarly.

3.2 Vibration Behaviour

A rotational velocity of 6000rpm is equivalent to 100Hz frequency. The eigenfrequency of neither the alpha- nor the beta-rotor approaches this frequency but is much over it. Tab. 1 sums up the eigenfrequency values.

The first eigenfrequency of both rotors is the same. This is clearly, because it effects only the coupler as fig. 12 shows. At the first eigenfrequency the coupler moves in the x-z-plane. The second eigenfrequency is a bit higher than the first one and effects also only the coupler. But this time it moves in

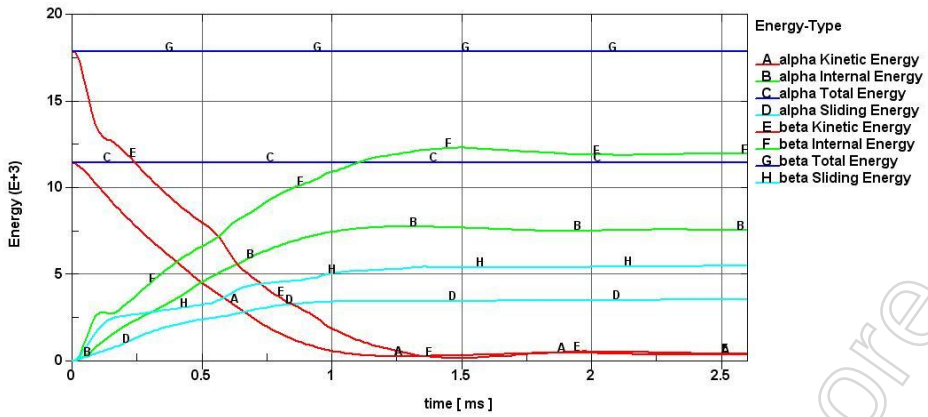

Figure 9: Energy Comparison

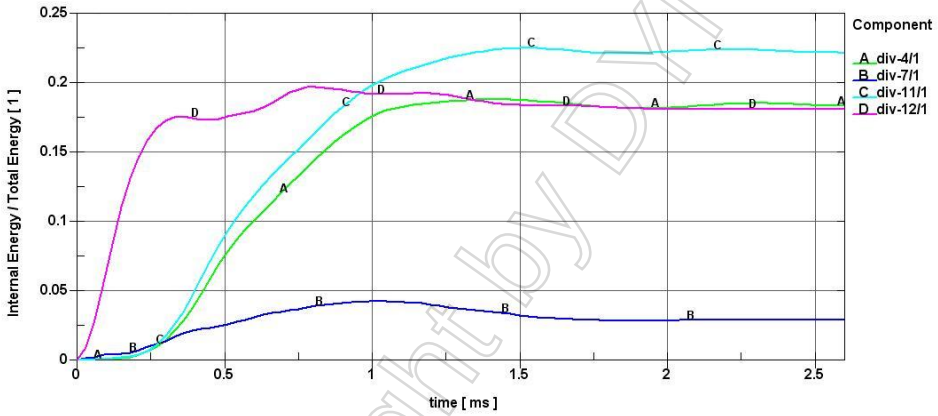

Figure 10: alpha-rotor Internal Energy

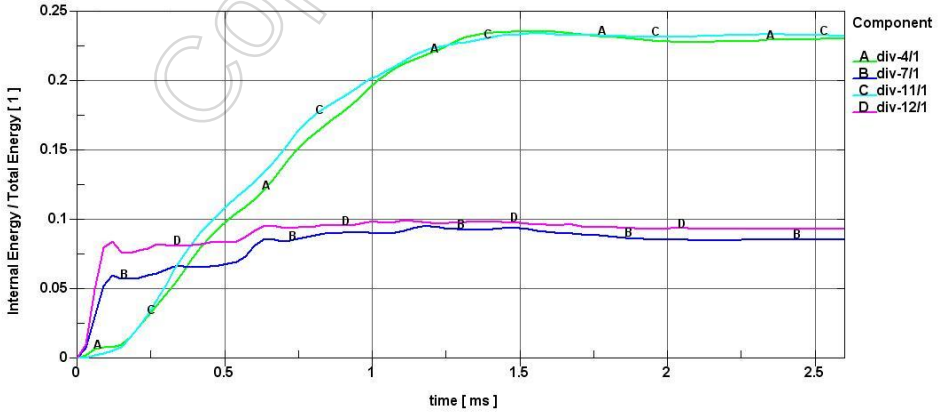

Figure 11: beta-rotor Internal Energy

the x-y-plane. First eigenfrequency of the piston is the third eigenfrequency of the rotors. The pistons differ in their respective first eigenfrequency. This is as expected because of the different weight. The alpha-rotor has got a eigenfrequency at 636.8Hz which is higher than the 577.8Hz of the beta-rotor. The eigenfrequency of something is inversely proportional to its mass. With less weight and constant stiffness, the eigenfrequency rises.

eigenfrequency	1^{st}	2^{nd}	3^{rd}	4^{th}	5^{th}
alpha-rotor	360.2	371.5	636.8	716.5	785.9
beta-rotor	358.9	372.5	577.8	728.5	752.4

Table 1: Eigenfrequency

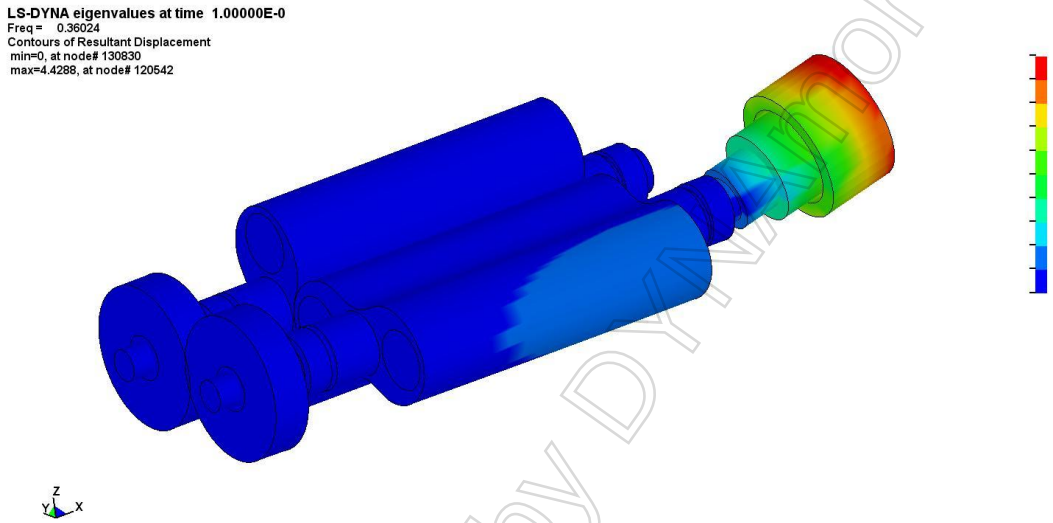

Figure 12: Eigenvalue Analysis, first eigenfrequency

4 Summary and Conclusions

The analysis show the potential of weight reduction. By making two holes into the piston, a weight reduction of more than 20% has been reached. The weight reduction can be risen even more by making a hollow piston. It is an optimization challenge to find the border of moving material from inside of the piston and still keeping the used stiffness.

With the existing state of stress it has been shown, that a material model is needed, which is able to consider triaxiality. A comparison of Mat_024 and Mat_120 has been made.

In the crash simulation two pistons with different geometry have been compared. The deformation of the shafts is decreased while the deformation of the pistons has risen. This is also shown by the energy history plot. The energy absorption of the shafts is reduced, the one of the pistons is risen. The total energy is reduced of about 25%. This effects lower forces on the bearings.

An implicit eigenvalue analysis has shown, that the eigenfrequencies are far over the operating frequency. The need of knowing the appearing frequencies in an industrial installation has been pointed out.

Finally it has been shown, how to combine crash analysis and vibration analysis by solving the problems with one code.

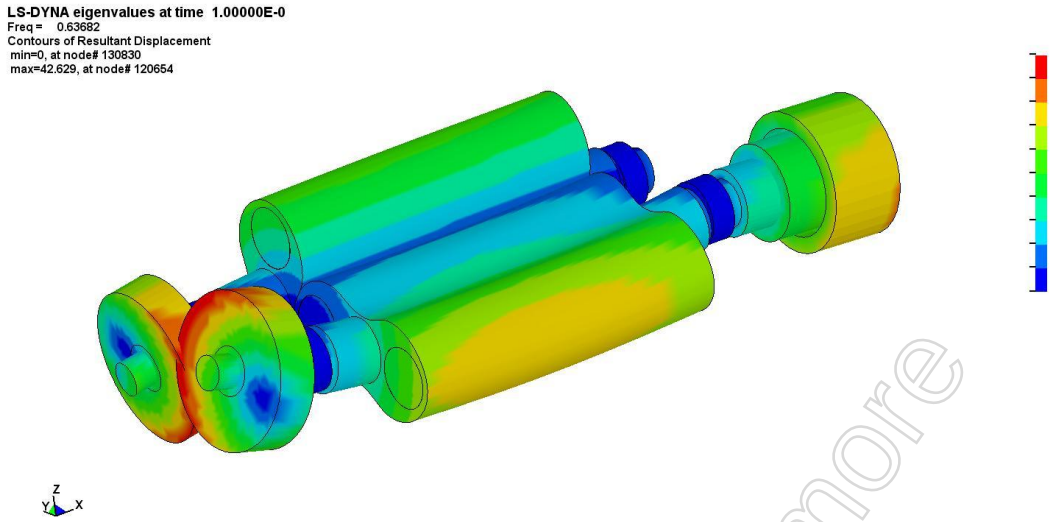

Figure 13: Eigenvalue Analysis, third eigenfrequency

5 Literature

[1] LS-DYNA, Theoretical Manual / User's Manual, Livermore Software Technology Corporation.

[2] Pfeiffer Vacuum GmbH: The Vacuum Technology Book. Asslar, 2008.

[3] Du Bois, P.A.; Kolling, S.; Feucht, M.; Haufe, A.: A comparative review of damage and failure models and a tabulated generalization. Proceedings of the 6th European LS-DYNA User's Conference, Gothenburg, Sweden, 2007.

[4] Johnson, G.R.; Cook, W.H.: Fracture characteristics of three metals subjected to various strains, strain rates, temperatures and pressures. Engineering Fracture Mechanics, vol.21, No.1, pp.31-48,1985.

[5] Neukamm, F.; Feucht, M.; Haufe, A.: Consistent damage modelling in the process chain of forming to crashworthiness simulations. Proceedings of the 7th LS-DYNA Forum, Bamberg, Germany, 2008.

[6] Ebelsheiser, H.; Feucht, M.; Neukamm, F.: On calibrating advanced damage models using sheet metal coupon test. Proceedings of the 7th LS-DYNA Forum, Bamberg, Germany, 2008.

[7] Feucht, M.; Sun, D.Z.; Erhart, T.; Frank, T.: Recent development and applications of the Gurson model. Proceedings of the 5th LS-DYNA Forum, Ulm, Germany, 2006.